A new age-dating model for cool main sequence stars that combines stellar evolution models with gyrochronology

ABSTRACT

By combining two different sets of observable stellar properties and dating methods that are sensitive to two different evolving processes in stars: core hydrogen burning and magnetic braking; it is possible to infer more precise and accurate ages than using either method in isolation. In this investigation, the observables of main sequence stars that are used to trace core hydrogen burning and stellar evolution on the Hertzprung-Russell diagram ($T_{\rm eff}$, [Fe/H], log g, parallax, apparent magnitude and photometric colors) are combined with their *Kepler* rotation periods, in a Bayesian framework, to infer stellar ages from *both* stellar evolution models and gyrochronology. We show that incorporating rotation periods into stellar evolution models significantly improves the precision of inferred ages. However, since ages predicted with gyrochronology are, in general, much more *precise* than isochronal ages but not necessarily more *accurate*, care must be taken to ensure either a) the gyrochronology relation being used is *extremely* accurate, or b) its precision is relaxed by introducing a mixture model or some intrinsic scatter or similar. In this pilot study we do not aim to produce a new state-of-the-art dating model, our goal is simply to explore the process of combining two heterogeneous dating methods. Combining methods like this can illuminate flaws in one or both, although without ground truth it can be difficult to identify the cause of inconsistencies. Although calibration is not the main purpose of this exploratory investigation and the parameters of our gyrochronology model are fixed, only a slight modification to our algorithm would be required to perform a calibration. Accompanying this publication is open source, packaged and documented code, that calculates stellar ages from spectroscopic parameters and/or apparent magnitudes, parallaxes and rotation periods.

1. Introduction

The formation and evolution of the Milky Way (MW) and the planetary systems within it are two topics of significant interest in astronomy today. Both of these fields require precise

and accurate ages of tens to hundreds of thousands of stars. Precise ages of red giant stars, some calculated from asteroseismology and some from spectroscopy have recently been used to explore the age distributions of stellar populations in the MW (*e.g.* ?). Red giants are highly luminous and can be observed to great distances, thus providing age information on the scale of tens of kilo-parsecs. Main sequence (MS) stars on the other hand, although fainter, are more numerous and so their ages may provide new insights into the formation and evolution of the Solar neighborhood. MS star ages are also of great interest for studying the formation and evolution of planetary systems. Almost all exoplanets discovered to date orbit MS stars and it is therefore *MS star* ages that are needed to study planet evolution. Unfortunately, the very property that makes MS stars good hosts for habitable planets also makes them difficult to date: they do not change substantially over time.

Unlike the spectra and photometric colors of red giants, MS star spectra and colors do not contain a significant amount of age information because they do not change rapidly. This is represented in the spacing of isochrones on a Hertsprung-Russell (HR) or color-magnitude diagram (CMD). On the MS, isochrones are tightly spaced and, even with very precise measurements of effective temperature and luminosity, the position of a MS star on the HR diagram may be consistent with range of isochrones spanning several billion years. On the giant branch however, isochrones are spread further apart, so that sufficiently precisely measured temperatures and luminosities may yield ages that are precise to within 20% or better. Look at typical age uncertainties from APOGEE. Asteroseismology can provide precise ages of *both* red giant and MS stars but due to the greater quantity of observations suitable for *red giant* asteroseismology, precise red giant asteroseismic ages outnumber MS ages. The typical periods of red giant acoustic pulsations are long (on the orders of hours to weeks) and can be detected using *Kepler*'s long cadence mode of one observation per thirty minutes, *Kepler*'s standard and most common observing mode. In addition, the amplitudes of red giant pulsations are typically very large, significantly greater than *Kepler*'s photometric noise floor. MS stars, on the other hand, oscillate with periods of just a few minutes and the long cadence *Kepler* observations, taken once every half-hour, are far above the Nyquist limit and not capable of resolving these pulsations. Asteroseismic measurements of MS stars can only be made when observed in *Kepler*'s short cadence mode of one observation every minute. However, since the amplitude of pulsation scales with stellar radius, the majority of stars with asteroseismic ages successfully measured using *Kepler* short-cadence observations, of which there are currently around 500 (Chaplin et al. 2014), are subgiants. Only ∼30 of these are truly on the MS. This may change soon however: *Kepler*'s short cadence light curves have recently been reprocessed and new, precise ages for the *all* stars observed in short cadence mode (around 2000 in the original *Kepler* mission) may be measured and made available soon.

The Sun's rotation period will vary by almost an order of magnitude over its MS lifetime due to magnetic braking. In contrast, luminosity and temperature are not sensitive age proxies for Sun-like stars, are often inferred indirectly, and can be difficult to infer precisely. In addition, the precision with which the luminosity and temperature of a star can be measured is highly sensitive to its distance and the amount of extincting dust along the line of sight. Stellar rotation periods are much more sensitive to age than luminosity or temperature and can be measured precisely, with little dependence on distance and none on extinction, directly from *Kepler* light curves. Gyrochronology, the dating method that uses stellar rotation periods, has the potential to provide MS star ages that are precise to around 20% (Epstein and Pinsonneault 2014). Due to the abundance of rotation periods of MS stars already provided by *Kepler*/*K2* and the many more expected from future photometric surveys, gyrochronology is one of the most readily available methods for inferring precise stellar ages and, as such, has gained interest over the last few years.

Magnetic braking in MS stars was first observed by Skumanich (1972) who, studying young clusters and the Sun, found that the rotation periods of Solar-type stars decay with the square-root of time. It has since been established that the rotation period of a star depends, to first order, only on its age and mass (*e.g.* Barnes 2003). This means that by measuring a star's rotation period and a suitable mass proxy (B-V color is commonly used), one can determine its age. The convenient characteristic of stars that allows their ages to be inferred from their *current* rotation periods and independently of their primordial ones, comes from the steep dependence of spin-down rate on rotation period (Kawaler 1989). This means that a star spinning with high angular velocity will experience a much greater angular momentum loss rate than a slowly spinning star. For this reason, no matter the initial rotation period of a Sun-like star, after around 500 million years stellar rotation periods appear to converge onto a tight sequence citation. After this time, the age of a star can be inferred, to first order, from its mass and rotation period alone; this is the principle behind gyrochronology.

The relation between age, rotation period and mass has been studied in detail CITATIONS, and several different models have been developed to capture the rotational evolution of Sun-like stars. Some of these models are theoretical and based on physical processes; modeling angular momentum loss as a function of the stellar properties as well as the properties of the magnetic field and stellar wind. Other models are empirical and capture the behavior of stars from a purely observational standpoint, using simple functional forms that can reproduce the data. Both types of model; theoretical and empirical, must be calibrated using observations. Even the theoretical models are highly sensitive to some stellar properties that are not measurable: mass-loss rate and magnetic field geometry, for example. However, despite significant advances in both types of model, the gyrochronology relations have not yet been finalized for two main reasons. Firstly, the rotational evolution of stars is complex

and not well understood. It is difficult to reproduce the trends in the data using the known physical processes acting within stellar interiors, surfaces and winds. It is also challenging to come up with an empirical model that is flexible enough to capture trends in the data. Secondly, there is a lack of suitable calibration stars with precisely measured ages, particularly at old ages. Old calibrators are especially important because new evidence suggests that rotational evolution goes through a transition at old age or, more specifically, at a large Rossby number, *Ro* (the ratio of rotation period to the convective overturn timescale). For example, old *Kepler* asteroseismic stars rotate more rapidly than expected given their age (*e.g.* Angus et al. 2015; van Saders et al. 2016). A new physically motivated gyrochronology model, capable of reproducing these data, was recently introduced (van Saders et al. 2016). It relaxes magnetic breaking at a critical Rossby number of around the Solar value, 2.1. This model predicts that, after stellar rotation periods lengthen enough to move stars cross this *Ro* threshold, stars stop spinning down and maintain a constant rotation period from then until they evolve off the MS. The implication is that the ages of stars with $Ro > 2.1$ cannot be measured from their rotation periods.

Despite recent advances in rotation-dating, such as the new *Ro* transition models (van Saders et al. 2016), there is substantial room for improvement in the gyrochronology relations. For example, there is, as yet no *fully* empirical gyrochronology model that includes a weakened magnetic braking law after the $Ro = 2.1$ transition. Empirical models have value as they are often more flexible than physical models and can capture trends in the data before the physical processes at work are fully understood. In addition, no single gyrochronology relation can reproduce the rotational behaviour of all open clusters; the relation between rotation period, age and mass varies from cluster to cluster in a way that cannot be captured by any current model. Again, this is related to the issue of model flexibility. Finally, more stars with precisely measured old ages are needed to confidently calibrate gyrochronology models at old ages. New asteroseismic calibrators will become available from reprocessed *Kepler* short cadence light curves, however significant numbers of suitable gyrochronology calibrators may not be accessible until after the European Space Agency's *PLATO* mission is launched.

The gyrochronology models that capture post *Ro*-threshold, rotational evolution (van Saders et al. 2016) are the current state-of-the-art in rotation dating. These models are expensive to compute and, just as with most isochrones and stellar evolution tracks, are usually pre-computed over a grid of stellar parameters in order to perform computionally tractable inference. Inferring ages using these models is similar to inferring an age using any set of isochrones, with the main difference being that rotation period is an additional dimension. Ages calculated using these models are therefore likely to be more precise than using rotation-free isochrones since rotation period provides an additional anchor-point for

the age of a star. We present here a complementary method that combines isochrones with an *empirical* gyrochronology model using a Bayesian framework. The methodology is related to the models described above (van Saders et al. 2016) in that both use a combination of rotation periods and other observable properties that track stellar evolution on the HR diagram in concert. The main difference is that the gyrochronology model used here is an entirely empirically calibrated one, as opposed to a physically derived one. One major advantage of using a physically motivated gyrochronology model over an empirically calibrated one is the ability to rely on physics to interpolate or extrapolate over parts of parameter space with sparse data coverage. However, rotational spin-down is a complex process that is not yet fully understood and currently no physical model can accurately reproduce all the data available. For this reason, even physically motivated gyrochronology models cannot always be used to reliably extrapolate into unexplored parameter space. Physical models, when calibrated to data can provide insight into the physics of stars however, if accurate and precise *prediction* of stellar properties is desired, empirical models can have advantages over physical ones. For example, the data may reveal complex trends that cannot be reproduced with our current understanding of the physical processes involved but may be captured by more flexible data-driven models. In addition, it is relatively straightforward to build an element of stochasticity into empirical models, *i.e.* to allow for and incorporate outliers or noisy trends. This may be particularly important for stellar spin down, which does not always seem to behave predictably. A further advantage of empirical models is that it can be extremely fast to fit them to data. We use a simple, deterministic gyrochronology model in this work, which, like any other gyrochronology model, cannot yet reproduce all the observed data. However, simple modifications could be made to this model to produce significant improvements, for example, by including instrinsic scatter and outliers. We leave these improvements for a future project. Ultimately, the model we present here will provide a baseline against which more physically motivated models can be compared.

This paper is laid out as follows. In section 2 we describe our new age-dating model and its implementation, in section 3 we test this model on simulated stars, cluster stars and asteroseismic stars, and in section 4 we discuss the implications of these tests and future pathways for development. Throughout this paper we use the word *'observables'* to describe the set of $T_{\rm eff}$, log g, observed bulk metallicity, parallax, photometric color and rotation period observations for a given star. We use the word *'parameters'* to refer to the physical properties of that star: age, mass, true bulk metallicity, distance and V-band extinction that *generate* the observables.

2. Method

A common approach to stellar age-dating is to make separate age predictions using separate sets of observables. For example, if a star's rotation period, parallax, and apparent magnitudes in a range of bandpasses are available, it is possible to predict its age from both gyrochronology and isochrone fitting separately. How these two age predictions are later combined is then a difficult choice. Is it best to average these predictions, to use the more precise of the two, or the one believed to be more accurate? The methodology described here provides an objective method for combining age estimates. There is, after all, only one age for each star. In Bayesian statistics, combining information from different models can be relatively simple, as long as the processes being modeled; those that generated the data, are independent. In this case, we are combining information that relates to the burning of hydrogen in the core (this is the process that drives the slow increase in $T_{\rm eff}$ and luminosity over time) with information about the magnetic braking history of a star (the current rotation period). We can assume that, to first order, these two processes are independent: the hydrogen fraction in the core does not affect a star's rotation period and vice versa. In practise, we can never be entirely sure that two such processes are independent but, at least within the uncertainties, any dependence here is unlikely to affect our results. If this assumption is valid, the likelihoods calculated using each model can be multiplied together.

The desired end product of this method is an estimate of the non-normalized posterior probability density function (PDF) over the age of a star,

$$p(A|\mathbf{m_x}, T_{\rm eff}, \log g, \hat{F}, P, \bar{\omega}), \tag{1}$$

where A is age, $\mathbf{m_x}$ is a vector of apparent magnitudes in various bandpasses (in our model $\mathbf{m_x} = [m_J,\ m_H,\ m_K]$), $\hat{F}$ is the *observed* bulk metallicity, P is the rotation period and $\bar{\omega}$ is parallax. In order to calculate a posterior PDF over age, we must marginalize over parameters that relate to age, but are not of interest in this study: mass (M), distance (D), V-band extinction (A_V) and the *inferred* bulk metallicity, F. The marginalization involves integrating over these extra parameters,

$$\begin{aligned} &p(A|\mathbf{m_x}, T_{\rm eff}, \log g, \hat{F}, P, \bar{\omega}) \qquad (2)\\ &\propto \int p(\mathbf{m_x}, T_{\rm eff}, \log g, \hat{F}, P, \bar{\omega}|A, M, D, A_V, F)\ p(A)p(M)p(D)p(A_V)p(F)dMdDdA_VdF. \end{aligned}$$

This equation is a form of Bayes' rule,

$$\text{Posterior} \propto \text{Likelihood} \times \text{Prior}, \tag{3}$$

where the likelihood of the data given the model is,

$$p(\mathbf{m_x}, T_{\rm eff}, \log g, \hat{F}, P, \bar{\omega}|A, M, D, A_V, F), \tag{4}$$

and the prior PDF over parameters is,

$$p(A)p(M)p(D)p(A_V)p(F). \tag{5}$$

Not all of the observables on the left of the '|' in the likelihood depend on all of the parameters to the right of it. For example, rotation period, P doesn't depend on V-band extinction, A_V. In our model, we make use of conditional independencies like this and use them to factorize the likelihood. Instead of the likelihood we wrote in equation 3, where every observable depends on every parameter, our model can be factorized as,

$$p(\mathbf{m_x}, T_{\rm eff}, \log g, \hat{F}, \bar{\omega}, C_{B-V}|A, M, D, A_V, F)\ p(P|A, C_{B-V}), \tag{6}$$

where we have introduced a new parameter, C_{B-V}, which is the $B-V$ color that is often used as a mass proxy in the literature. In our model C_{B-V} is not measured but *inferred*: it is a latent parameter. We infer C_{B-V} because all *Kepler* stars have 2MASS photometry in J, H and K bands but do not all have B and V band colors. However, the gyrochronology model we use is calibrated to B-V color, not J-K or otherwise. A probabilistic graphical model (PGM) depicting the joint probability over parameters and observables is shown in figure 1. It describes the conditional dependencies between parameters (in white circles) and observables (in grey circles) with arrows leading from the causal processes to the dependent processes. For example, it is the mass, age, metallicity, extinction and distance that determines the observed spectroscopic properties ($T_{\rm eff}$, log g and [Fe/H]) and apparant magnitudes (m_J, m_H and m_K). These parameters also determine the B-V color of a star. In turn, it is a star's age and B-V color that determine its rotation period. Note that, written this way, stellar rotation periods do not directly depend on stellar mass. Mass determines C_{B-V} and C_{B-V}, along with age determines rotation period. The purpose of this PGM is not to depict the physical realities of stellar evolution, it is only a visual description of the structure of the model we use here. Breaking up the problem this way allows us to efficiently join isochronology and gyrochronology and infer the joint age of a star from all its observables. It may well be that rotation period depends directly on mass and metallicity in reality, but it is more practical for us to assume that these dependencies are weak enough not to significantly affect the ages that we ultimately infer.

The factorization of the likelihood described in equation 6 and depicted in figure 1 allows us to multiply two separate likelihood functions together: one computed using an isochronal model and one computed using a gyrochronal model. We assume that the probability of observing the measured observables, given the model parameters is a Gaussian and that the observables are identically and independently distributed. These assumptions allow us to use Gaussian likelihood functions. The isochronal likelihood function is,

$$\mathcal{L}_{\rm iso} = p(\mathbf{m_x}, T_{\rm eff}, \log g, \hat{F}, \bar{\omega}, C_{B-V}|A, M, D, A_V, F) \tag{7}$$

Fig. 1.— A probabilistic graphical model (PGM) showing the conditional dependencies between the parameters (white nodes) and observables (gray nodes) in our model. θ is a vector of *parameters*: mass, observed bulk metallicity, distance and V-band extinction; and $\mathbf{O}$ is a vector of *observables*: apparent magnitudes, effective temperature, surface gravity, observed bulk metallicity, and parallax. The observables, $\mathbf{O}$, are determined by the parameters, A and θ. C_{B-V} is a latent parameter that is also determined by the parameters A and θ. In our model, the rotation period observable, P, is determined *only* by the age, A, and color C_{B-V} parameters. The dependencies of observables on parameters and parameters on parameters are indicated by arrows that start at a 'parent' node and end at the dependent observable, or 'child' node. In our model, rotation period does not directly depend on distance, extinction, metallicity or mass, only age and B-V color. This PGM is a representation of the factorized joint PDF over parameters and observables which is written in equation 6.

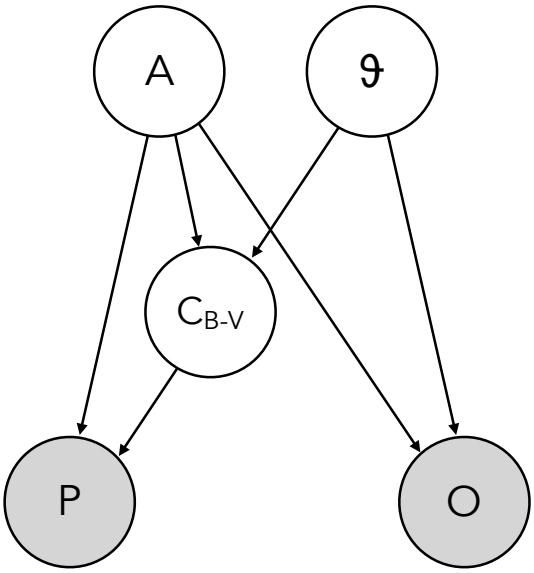

$$= \frac{1}{\sqrt{(2\pi)^n \det(\Sigma)}} \exp\left(-\frac{1}{2}(\mathbf{O_I} - \mathbf{I})^T \Sigma^{-1} (\mathbf{O_I} - \mathbf{I})\right),$$

where $\mathbf{O_I}$ is the vector of n observables: $T_{\rm eff}$, log g, $\hat{F}$, $\bar{\omega}$, m_j, m_h and $m_k$and Σ is the covariance matrix of that set of observables. $\mathbf{I}$ is the vector of *model* observables that correspond to a set of parameters: A, M, F, D and A_V, calculated using an isochrone model. We assume there is no covariance between these observables and so this covariance matrix consists of individual parameter variances along the diagonal with zeros everywhere else. The gyrochronal likelihood function is,

$$\mathcal{L}_{\rm gyro} = p(P|A, C_{B-V}) \tag{8}$$
$$= \frac{1}{\sqrt{(2\pi)\det(\Sigma_P)}} \exp\left(-\frac{1}{2}(\mathbf{P_O} - \mathbf{P_P})^T \Sigma^{-1} (\mathbf{P_O} - \mathbf{P_P})\right),$$

where $\mathbf{P_O}$ is a 1-D vector of observed rotation periods, $\mathbf{P_P}$ is the vector of corresponding predicted rotation periods, calculated using the vector of inferred ages and C_{B-V} values predicted by the isochronal model. The full likelihood function used in our model is the product of these two likelihood functions,

$$\mathcal{L}_{\rm full} = \frac{1}{\sqrt{(2\pi)^n \det(\Sigma)}} \exp\left(-\frac{1}{2}(\mathbf{O_I} - \mathbf{I})^T \Sigma^{-1} (\mathbf{O_I} - \mathbf{I})\right) \tag{9}$$
$$\times \frac{1}{\sqrt{(2\pi)\det(\Sigma_P)}} \exp\left(-\frac{1}{2}(\mathbf{P_O} - \mathbf{P_P})^T \Sigma^{-1} (\mathbf{P_O} - \mathbf{P_P})\right).$$

We place priors over the model parameters A, M, F, D and A_V. These priors represent our 'prior beliefs' about the values these parameters will take, before we use the data to update those beliefs via a likelihood and produce a 'posterior' belief about their values. These priors are described in the appendix.

The gyrochronology model we use to predict P_P is,

$$P = A^{\eta} \alpha (B - V - \delta)^{\beta}, \tag{10}$$

where P is rotation period in days, $B - V$ is a star's color, A is stellar age in Myrs and η, α, β and δ take values 0.55, 0.4, 0.31 and 0.45 respectively. This functional form was introduced by (Barnes 2007) and the parameter values are adopted from the recalibration performed in Angus et al. (2015), which is based on young cluster stars and old asteroseismic stars and incorporates a Gaussian mixture model that prevents outliers from influencing the fit. Although this model has been calibrated using a number of cluster stars, it does not provide a good fit to any individual cluster. No current gyrochronology model is able to capture the behavior of rotation as a function of color and age for individual benchmark clusters: the shape of this relation is different in each. The models are not flexible enough to capture inter-cluster differences in rotational evolution. For this reason, we explored the

rotational evolution of a *single* cluster, in order to produce a best-case model and demonstrate the potential of rotation-dating in a case where the model is perfectly accurate. We chose Praesepe as it is a relatively old open cluster ($\sim$ 650 Myrs citation), meaning its Solar-type members have converged onto the rotational main sequence, and it is relatively compact on the sky so many of its members were observed during a single *K2* campaign. In fact, Praesepe was repeatedly observed by *K2*, in Campaigns 5, 16 and 18, however we only use rotation periods published from the analysis of Campaign 5 in this work.

We used a three-dimensional polynomial model to predict rotation period as a function of *Gaia* color and age for Praesepe and the Sun. This model consists of a 4th order polynomial in logarithmic Gaia color: $G_{Bp} - G_{Rp}$, which we write as C_G for simplicity, and a 1st order polynomial (a straight line) in logarithmic age. We switched to using $G_{Bp} - G_{Rp}$ because, due to the $\sim$ billion stars observed by *Gaia*, it is now the most abundant and widely available photometric color. Our gyrochronology likelihood function is designed to compare observed rotation period to predicted rotation period. For this reason the gyrochronology model we used must predict rotation period as a function of age and color. However, when *calibrating* the gyrochronology model, we chose to make *age* the dependent variable because the uncertainties on age are much greater than the uncertainties on rotation period. Since we are using a linear model, the relation is easily invertable. We fitted the following model to Praesepe members:

$$\log_{10}(A) = a + b\log_{10}(C_G) + c\log_{10}^2(C_G) + d\log_{10}^3(C_G) + e\log_{10}^4(C_G) + f\log_{10}(P) \quad (11)$$

where P is rotation period in days, C_G is Gaia color, A is stellar age in years and the lower case letters are free parameters which we fitted to the data using linear least squares. We adopted an age for Praesepe of 650 million years citation, a Solar age of 4.56 Gyr citation, and a Solar rotation period of 26 days citation. The Sun's color in the Gaia color bandpasses, $G_{Bp}-G_{Rp}$, is 0.82 (Casagrande and VandenBerg 2018). We found best-fit values: $a = 7.37 \pm 0.03, b = -1.4 \pm 0.1, c = 5.0 \pm 0.8, d = -34 \pm 3, e = 66 \pm 14$, and $f = 1.49 \pm 0.02$. Rotation periods for Prasepe were obtained from **?** and their *Gaia* colors were obtained by crossmatching their sky-projected positions with the *Gaia* DR2 catalog. We inverted this relation to predict rotation period as a function of color and age,

$$\log_{10}(P) = \frac{\log_{10}(A) - a - b\log_{10}(C_G) - c\log_{10}^2(C_G) - d\log_{10}^3(C_G) - e\log_{10}^4(C_G)}{f}. \quad (12)$$

We used both equations 11 and 12 to predict the ages of individual Praesepe stars from their rotation periods and apparent magnitudes in section 3.

It was recently shown that a simple power law in age does not provide a good fit to old asteroseismic stars (**?**van Saders et al. 2016). It is hypothesized that the magnetic braking of

these old stars has ceased and cannot be modeled with a Skumanich-like spin-down law (van Saders et al. 2016). In future, the above model could and should be updated to include a more flexible treatment of rotation period as a function of age in order to account for the change of slope in the relation. Until then, this method should only be used for stars with Rossby number below 2.1 (van Saders et al. 2016), *i.e.* their ratio of rotation period to convection overturn time ($P/\tau = Ro$) does not exceed 2.1. In this work we are chiefly concerned with introducing a new framework where rotation periods are modeled *simultaneously* with isochronal features. Although this gyrochronology model does not provide a good fit to all the available data, we reiterate that no single model *is* able to reproduce all the data, and that there is utility in using such a simple, linear, empirical model like this. Again, we are not attempting to improve gyrochronology models in this work: in this paper we are more concerned with introducing a new approach to modeling stellar ages, however, our method is highly flexible and modular and an improved gyrochronology model could easily be swapped in for this one in future. Our model allows a linear combination of other, *physical* parameters to be used to predict age from rotation period, like $\log g$, metallicity and mass. In future, it may be better to model stars in physical rather than observable parameter space.

To calculate $\mathbf{I}$, the vector of predicted isochronal observables, we use the `isochrones.py` *python* package which has a range of functionalities relating to isochrone fitting. The first of the `isochrones.py` functions we use is the likelihood function of equation 8. The `isochrones.py` likelihood function accepts a dictionary of observables which can, but does not *have* to include, all of the following: $T_{\rm eff}$, $\log\ g$, [Fe/H], parallax and apparent magnitudes in a range of colors, as well as the uncertainties on all these observables. It then calculates the residual vector $(\mathbf{O_I} - \mathbf{I})$ where $\mathbf{O_I}$ is the vector of observables and $\mathbf{I}$ is a vector of corresponding predicted observables. The prediction is calculated using a set of isochrones (we use the MIST models **?**), where the set of *model* observables that correspond to a set of physical parameters is returned. This requires interpolation over the model grids since, especially at high dimensions, it is unlikely that any set of physical parameters will exactly match a precomputed set of isochrones. The observables that correspond to a set of physical parameters (age, mass, etc) go into $\mathbf{I}$ and the `isochrones.py` likelihood function returns the result of equation 8. The second `isochrones.py` function we use is one that querys the best-fit isochrone model chosen to predict $\mathbf{I}$, in order to predict the corresponding C_{B-V} for that star. This color is then used to calculate the gyrochronal likelihood function of equation 9.

The inference processes procedes as follows (as a reminder, we use *observables* to refer to the data: $T_{\rm eff}$, $\log\ g$, etc and *parameters* to refer to the model parameters: age, mass, etc). First, a set of parameters: age, mass, true bulk metallicity, distance and extinction, as well as observed values of $T_{\rm eff}$, $\log\ g$, bulk metallicity, 2MASS colors and parallax ($\mathbf{O_I}$) for

a single star are passed to the isochronal likelihood function (equation 8). Then, a set of *model* values of $T_{\rm eff}$, log g, bulk metallicity, 2MASS colors and parallax (**I**) that correspond to that set of parameters are calculated by `isochrones.py`. The isochronal log-likelihood, $\ln(\mathcal{L}_{\rm iso})$, is then computed for these parameter values. The same age that was passed to the likelihood function, and the C_{B-V} corresponding to it, along with the observed rotation period, are then passed to the gyrochronal likelhood function (equation 9). The gyrochronal log-likelihood, $\ln(\mathcal{L}_{\rm gyro})$, is computed. The full log-likelihood is then calculated,

$$\ln(\mathcal{L}_{\rm full}) = \ln(\mathcal{L}_{\rm iso}) + \ln(\mathcal{L}_{\rm gyro}), \tag{13}$$

and added to the log-prior to produce a single sample from the posterior PDF.

We sampled the joint posterior PDF over age, mass, metallicity, distance and extinction using the affine invariant ensemble sampler, `emcee` (**?**). We used 24 walkers and sampled the posterior PDF until 100 *independent* samples were obtained. We estimated the autocorrelation length, indicating how many steps are taken per independent sample, after every 100 steps using the autocorrelation tool built into `emcee`. We stopped obtaining samples when either *both* 100 times the autocorrelation length was reached *and* the change in autocorrelation length over 100 samples was less than 0.01, or the maximum of 100,000 samples was obtained. This allowed use to continue obtaining samples from the posterior This provided an average of ... non-independent samples. The method described above is trivially parallelizable, since the inference proccess for each star can be inferred on a separate node. Running our code on a cluster, we found that a posterior PDF can be estimated for a single star in around one minute.

3. Results

In order to demonstrate the functionality of our method, we conducted two tests. In the first we simulated a set of observables from a set of fundamental parameters for a few hundred stars using the MIST (**?**) stellar evolution models. In the second we tested our model by attempting the measure the ages of stars in the Praesepe open cluster who's age has been measured precisely because it is an ensemble of coeval stars with the same metallicity; a single stellar poplulation, and its age can be established through isochrone fitting and MS turn-off.

For the first test we began with a set of 1000 stars and drew masses, ages, bulk metallicities, distances and extinctions at random from the following uniform distributions:

$$M \sim U(0.5, 1.5)\ [M_\odot] \tag{14}$$
$$A \sim U(0.5, 14)\ [\text{Gyr}] \tag{15}$$
$$F \sim U(-0.2, 0.2) \tag{16}$$
$$D \sim U(10, 1000)\ [\text{pc}] \tag{17}$$
$$A_V \sim U(0, 1). \tag{18}$$

T_{eff}, log g, $\hat{F}$, m_x, $\bar{\omega}$ and B-V were then generated using these stellar parameters with the MIST stellar evolution models (**?**) and rotation periods, P were generated from the gyrochronology relation in equation 10 with age, A, and B-V. We then performed cuts on these simulated stars to remove evolved stars and stars that are too hot. The rotation periods of evolved stars, defined here to be those with log g ¿ 4.5 begin to increase as soon as they turn off the MS and their radii start to enlarge and cannot be modeled with the gyrochronology relation of equation 11. In addition, hot stars (defined as 6250 K ¡ T_{eff}) cannot be modeled using equation 11 because their convective envelopes are extremely shallow and their magnetic fields are weaker, leading to a lack of magnetic braking. The rotation periods of these stars do not increase substantially during their time on the MS. After performing these cuts, 649 update stars remained in the sample of simulated stars. We took two approaches to inferred the ages of these simulated stars: firstly using *only* a stellar evolution model, and secondly using a stellar evolution model *combined with* a gyrochronology model. For all stars, our initial guesses for the parameters are $M = 1M_\odot$, $A = 1$ Gyr, $F = 0$, $D = 500$ pc and $A_V = 0.1$.

Figure 2 shows the results of using a stellar evolution model model to estimate the posterior PDFs over the stellar ages of simulated stars. The rotation periods of stars have not been incorporated into this model: these posterior PDFs were obtained by isochrone fitting only, using the likelihood function in equation 8. In most cases ages are only weakly

Fig. 2.— The results of a test in which we simulated observable properties of stars with the same model we used to infer their properties. In this experiment we used *only* stellar evolution models to infer ages; we did not use rotation periods. For results where we used *both* stellar evolution models *and* gyrochronology, see figure 3. The true age, used to produce associated observables is shown on the x-axis, and the ages we inferred are shown on the y-axos. This figure shows the posterior PDFs over stellar age for each of the simulated stars as a 'violin plot', where samples from the posterior are plotted vertically as a smooth, symmetric function. The widths of these functions indicates the probability over age: wider regions represent more probable ages. The median values of the posterior PDFs are plotted as solid horizontal lines. This figure demonstrates that when only stellar evolution models are used to infer ages for field MS stars, the resulting predicted ages are extremely imprecise.

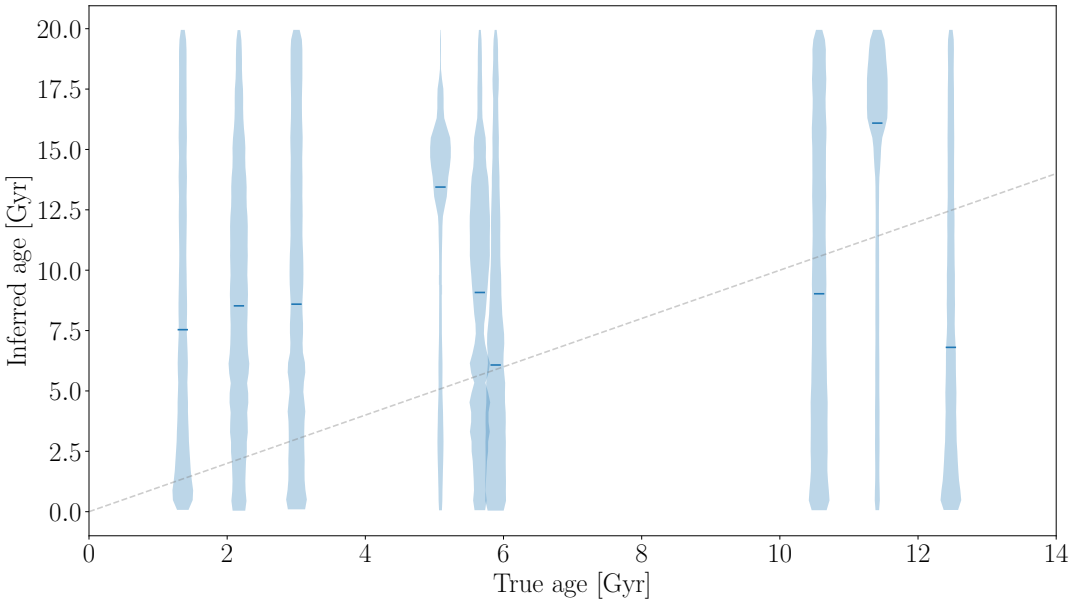

Fig. 3.— The results of a test in which we simulated observable properties of stars with the same model we used to infer their properties. In this experiment we used *both* stellar evolution models to rotation periods to infer ages. For results where we used stellar evolution models *only*, see the previous figure (figure 2). The true age, used to produce associated observables is shown on the x-axis, and the ages we inferred are shown on the y-axis. This figure shows the posterior PDFs over stellar age for each of the simulated stars as a 'violin plot', where samples from the posterior are plotted vertically as a smooth, symmetric function. The widths of these functions indicates the probability over age: wider regions represent more probable ages. The median values of the posterior PDFs are plotted as solid horizontal lines. This figure demonstrates that when rotation periods (gyrochronoloy) *and* stellar evolution models are used to infer the ages of field MS stars, the resulting predicted ages relatively precise; much more precise than when using stellar evolution models alone.

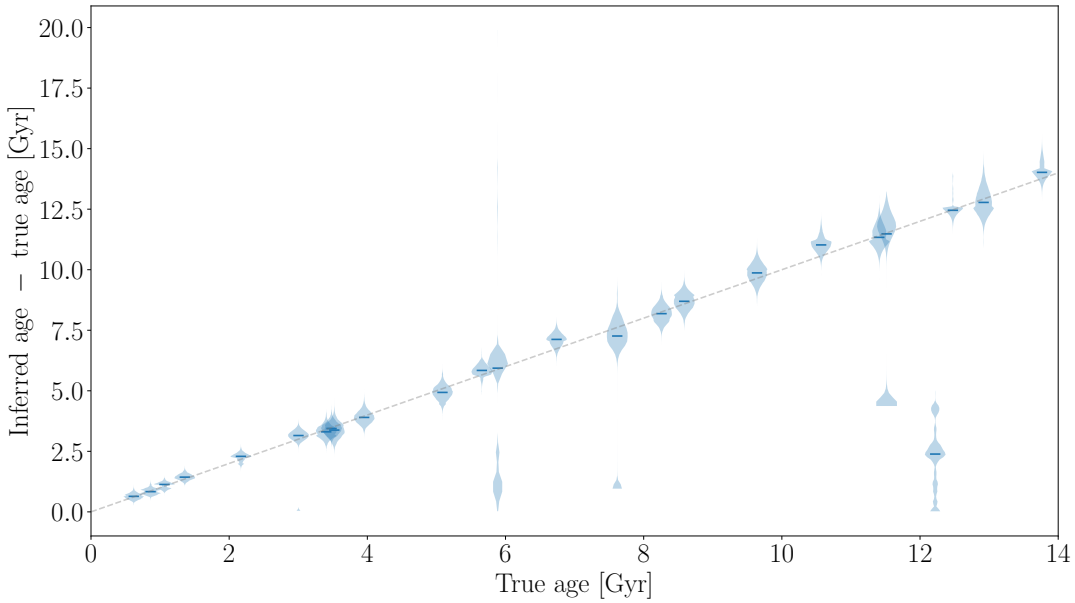

constrained by the stellar evolution models. In some cases there is no constraint on the stellar age: the age of the star is consistent with all ages from 0-14 Gyrs. The reason for this is that the temperatures and luminosities of stars do not change very much on the main sequence. The isochrones are tightly spaced in the MS region of the HR-diagram and, as a result, even precisely measured temperatures and luminosities often do not yield precise ages. Figure 3 shows the results of using a stellar evolution, combined with a gyrochronology model. These ages have been inferred using the likelihood of equation 13. Again, the true stellar ages are plotted on the x-axis and the posterior PDFs of the inferred ages are plotted on the y-axis. Here, unlike the case where only stellar evolution models were used, the recovered ages are precise. This is because gyrochronology isochrones (or gyrochrones) are more widely separated relative to the observational uncertainties than the isochrones used above. Put another way, the rotation periods of two stars of different ages and the same mass will have rotation periods that differ significantly – almost certainly more than the observational uncertainty on rotation period. On the other hand, two stars of the same mass and different age are likely to have extremely similar luminosities and temperatures and the differences between these properties are likely to be smaller than the observational uncertainties.

Figure **??** demonstrates the results of inferring ages using rotation periods only, and this illustrates why the combination of isochronal and gyrochronal ages is so precise: almost all this precision comes from rotation periods. This simulation experiment is unrealistic for two main reasons: firstly, we simulated data from the same gyrochronology model we used to infer ages and so the results will be perfectly accurate by design. Secondly, we simulated data without any intrinsic scatter built into the gyrochronology model; it is a deterministic model. This means that a rotation period and color predicts a corresponding single-valued age, rather than a probability distribution over ages. This is unrealistic given observations of open clusters who's members clearly show excess scatter in their rotation periods, particularly for less massive stars. These results look precise and accurate, but this is misleading. Inaccuracies would arise if the gyrochronology model was incorrect or poorly calibrated in all parts of parameter space and imprecision would arise if intrinsic scatter were built into the gyrochronology model. The result of using a deterministic model, such as the one used in this experiment, is that the uncertainties on stellar ages will be unrealistically small.

In this experiment, we compared the precision of MS field star ages inferred with stellar evolution models only, and with stellar evolution models *combined* with gyrochronology models. We showed that including gyrochronology in the stellar evolution model results in much more precise age predictions. We have not yet made any statement about accuracy however; the above experiment produces accurate ages by construction. In order to test the

potential of this method to produce accurate results, we test our model on real data in the following section.

In order to test our model on real stars with known ages, we selected a sample of cluster stars with precisely measured ages from ensemble isochrone fitting and main sequence turn off. The ages of open clusters can be measured much more precisely than field stars for two main reasons. Firstly, the stars have the same age (to within a few million years), so the age of a cluster can be inferred with an increased precision that is proportional to the square root of the number stars, relative to a single star case. In addition, stars in the same cluster form (we assume) from the same molecular cloud and therefore have the same metallicity. Since cluster stars have the same metallicity and age, stars fall on the same isochrone and the main sequence turn off can be identified. We compiled rotation periods and Gaia photometry and parallaxes for members of Praesepe, a 650 Myr cluster. We chose Praesepe because it is relatively tightly clustered on the sky and many of its members were therefore targeted in a single *K2* campaign, from which it was possible to measure rotation periods via frequency analysis of member's light curves (**?**). We crossmatched N Praesepe members with measured rotation periods (**?**), with the Gaia DR2 catalog Gaia DR2 citation, using a 5" search radius. The result was a sample of N stars with rotation periods, parallaxes and *Gaia* G, G_{BP} and G_{RP} -band photometry. Figure **??** shows the rotation periods of Praesepe members as a function of their dust-corrected *Gaia* $G_{Bp} - G_{Rp}$ colors. We used the `dustmaps python` package to calculate dust extinction along the line of sight to these stars. The filled blue circles show the FGK stars on the 'rotational main sequence' that were used to calibrate a relation between rotation period and color for this cluster.

In order to fit a period-color relation to these data we restricted the sample of cluster stars to the color range, $0.56 < G_{Bp} - G_{Rp} < 3$ in order to remove early F and late M dwarfs whos' rotation periods do not fall on the 'gyrochronology main sequence'. Although it *may* be possible to crudely predict the ages of these stars (at least the M dwarfs) from their rotation periods, the age-rotation-color relation for these stars is very different to the FGK star relations and is not the focus of this paper. In addition, we removed rapidly rotating stars from the sample since, although modeling outliers is important and consequential for gyrochronology in general, the goal of this paper is not to produce a perfect gyrochronology that reproduces stochasticity in the data, just a simple function that fits the rotational main sequence of Praesepe. In future we plan to update the gyrochronology models to include M dwarfs, and the outlying rapid rotators using a mixture of Gaussians. Similarly, we used only Praesepe in this study because the period-color relations of each open cluster with rotation periods has a different shape. This is likely due to differences in metalicities, incomplete or noisy membership lists and differences in rotation period measurement algorithms. A global gyrochronology calibration, using all cluster data is planned for the future but, again,

is beyond the scope of the project presented here. The rotation periods of the Praesepe members in the restricted color range and with outliers removed are plotted against their *Gaia* colors in figure **??**. We used linear least squares to fit a linear model to Praesepe and the Sun. A 4th order polynomial in $\log(G_{BP} - G_{RP})$ and a straight line in log(Age [yrs]) was fit to reproduce log(rotation period [days]).

$$\log(P) = a + b\log(C_G) + c\log^2(C_G) + d\log^3(C_G) + e\log^4(C_G) + f\log(A), \qquad (19)$$

were P is period, C_G is $GaiaG_{Bp} - G_{Rp}$ color, and A is age.

The age of each Praesepe member was inferred using both gyrochronology models: the legacy model of equation **??** and the Praesepe model of equation 3. This exercise is not designed to test one gyrochronology model against another: the model fit to the Praesepe data will provide a better age prediction by design, as the legacy model was fit to number of clusters at once. The point of this exercise is to show how precise gyrochronology could be if the perfect model is used. We did not force the cluster members to have the same age since the aim of this experiment was to reveal the precision and accuracy of our method by quantifying the level of scatter in our predicted ages and identifying regions of parameter space where the ages deviate from the established age for Praesepe.

The results are shown in figure **??** which follows the same layout as figure **??**. The top panels shows the ages inferred using an isochrone-only model, the middle shows a gyrochrone-only model and the bottom shows an isochrone plus gyrochrone model. Once again, the top panel demonstrates that using an isochrone model alone produces imprecise ages. The middle panel shows ages recovered using only a gyrochronal model and it reveals inaccuracies in the gyrochronology relation used here.

The bottom panel, once again, demonstrates the power of using both isochronal and gyrochronal models together to provide a balance of precision and accuracy.

Fig. 4.— The rotation periods of Praesepe members and the Sun, plotted against their *Gaia* colors ($G_{Bp} - G_{Rp}$) in logarithmic space. We fit a 4th order polynomial to these data in order to predict rotation periods from *Gaia* colors, and a 1st order polynomial (a straight line) in age. The result of this fit is plotted on top of the data at the ages of Praesepe and the Sun.

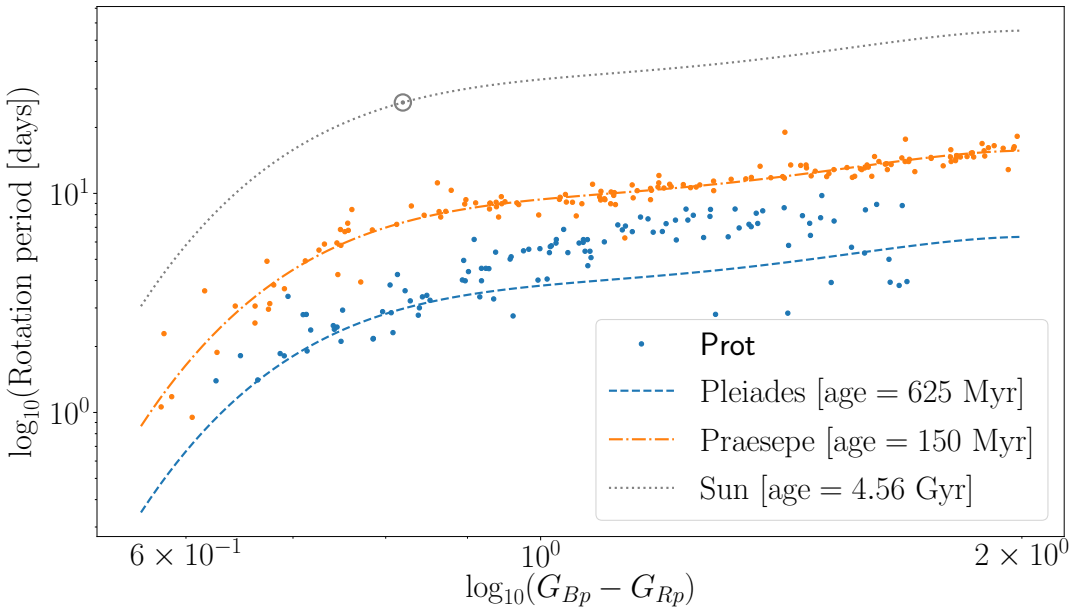

4. Discussion

In the previous section we demonstrated that modeling the ages of stars using isochrones *and* gyrochronology can result in more precise and accurate ages than using either isochrone fitting or gyrochronology alone.

Isochrone fitting and gyrochronology are extremely complementary because gyrochronology is more precise where isochrone fitting is less precise and vice versa. Age precision is determined by the spacing of isochrones or gyrochrones: in regions where iso/gyrochrones are more tightly spaced, ages will be less precise. Isochrones get less tightly spaced (and more precise) at larger stellar masses and gyrochrones get more tightly spaced (and less precise) at larger stellar masses. Figure **??** shows our simulated star sample on an H-R diagram. Points are positioned by their true properties, not their inferred ones, and colored by their age *precision* as calculated using isochrones and gyrochronology. Paler stars have less precise inferred ages.

The method we present here will be useful for a large number of stars: tens-of-thousands *Kepler* stars already and many more from *TESS*, *LSST*, *WFIRST*, *PLATO*, *Gaia*, *PanSTARRS* and more. However, there are also several types of star for which gyrochronology is, in general, *not* useful. This list includes: stars with thin convective envelopes, more massive than around 1 $M_{\odot}$; fully convectives stars, less massive than around 0.3 $M_{\odot}$; evolved stars with log g less than around 4.5; stars that haven't converged onto the rotational main sequence, *i.e.* those younger than around 500 Myrs; stars who have ceased magnetic braking, *i.e.* those with *Ro* greater than around 2.1; synchronised binaries who's rotation periods are locked to their orbital periods; and other classes of gyrochronal outliers. Since many stars with measurable rotation periods do not have precise spectroscopic properties, it is not always possible to tell whether a star falls within these permissable ranges of masses, surface gravities and rossby numbers. In addition, any given star, even if it does meet the criteria for mass, evolutionary stage, age, binarity, etc, may still be a rotational outlier. Rotational outliers are often seen in clusters (see *e.g.* **?**). In any case where a star's age is not truly represented by its rotation period, its isochronal age will be in tension with its gyrochronal one. However, given the precision of the gyrochronal technique, the gyrochronal age may dominate over the isochronal one. Figure **??** shows the posterior PDF for a star with a misrepresentative rotation period. This star is rotating more rapidly than its age and mass indicate it should, so the gyrochronal age of this star is under-predicted. Situations like this are likely to arise relatively often, partly because rotational spin-down is not a perfect process and some unknown physical processes can produce outliers, and partly because misclassified giants, hot stars, M dwarfs or very young or very old stars will not have rotation periods that relate to their ages in the same way. In addition, measured rotation periods may not always be

accurate and in many cases, due to aliasing, can be a harmonic of the true rotation period. One of the more common rotation period measurement failure modes is to measure half the true rotation period. The best way to prevent an erroneous or outlying rotation period from resulting in an erroneous age measurement is to *allow* for outlying rotation periods using a mixture model.

Throughout this manuscript we have referred to the 'accuracy' of the isochronal models. In reality though, stellar evolution models are not 100% accurate and different stellar evolution models, *e.g.*, MIST, Dartmouth, Yonsei-Yale, etc will predict slightly different ages. The disagreement between these models varies with position on the HR diagram, but in general, ages predicted using different stellar evolution models will vary by around 10%. We use the MIST models in our code because they cover a broader range of ages, masses and metallicities than the Dartmouth models.

Our focus so far has been on stellar age because this is the most difficult stellar parameter to measure. However, if the age precision is improved, then the mass, [Fe/H], distance and extinction precision must also be improved, since these parameters are strongly correlated and co-dependent in the isochronal model. Figure **??** shows the improvement in relative precision of mass measurements from our simulated star sample.

5. Conclusion

We have presented a statistical framework for joining together observations of different stellar properties that relate, via different evolutionary processes, to stellar age. Specifically, we combine information used to place stars on an isochrone in an HR diagram: $T_{\rm eff}$, log g, observed bulk metallicity, parallax and photometric colors with rotation periods, used to date stars via their magnetic braking history. The two methods of ischrone fitting and gyrochronology are simply combined by taking the product of two likelihood functions: one that contains an isochronal model and the other a gyrochronal one. The isochronal model is based on the MIST stellar evolution model (**?**) and computed using `isochrones.py`. The gyrochronal model is a simple 2-dimensional power-law relation between rotation period, B-V color and age. It is based on the functional form first introduced by Barnes (2003) and later recalibrated by Angus et al. (2015).

We tested this age-dating model on simulated data, cluster stars and asteroseismic stars with precisely measured ages. The age of the Hyades is generally measured using stellar evolution/isochrone models where the ensemble of stars at the same age but a *range of masses* allows a very precise isochronal age to be inferred. In particular, this allows the main sequence-turn off to be identified which, since it appears as a sharp feature in a mono-age population, allows the age of the population to be precisely inferred. We found that this model predicts ages that are an order of magnitude more precise than using isochrone fitting alone. However, we caution users of this method that our choice of gyrochronology model is not suitable for stars outside a specific range of stellar parameters, described in the text.

In the future we hope to make several improvements to the gyrochronology relation used here, including, allowing for outliers via a mixture model, including intrinsic scatter and/or replacing the power-law with a semi-parametric model.

The code used in this project is available as a documented *python* package called `chronology`. It is available for download on Github or through Pypi (pip install chronology). The documentation is available at readthedocs.... The exact version used to produce the results here is available under add github hash.

6. Appendix

Priors

We use the default priors in the `isochrones.py` *python* package. The prior over age is,

$$p(A) = \frac{\log(10)10^A}{10^{10.5} - 10^8}, \quad 8 < A < 10.5. \tag{20}$$

where A, is $\log_{10}$(Age [yrs]). The prior over mass is uniform in natural-log between -20 and 20,

$$p(M) = U(-20, 20) \tag{21}$$

where M is ln(Mass $[M_\odot]$). The prior over true bulk metallicity is based on the galactic metallicity distribution, as inferred using data from the Sloan Digital Sky Survey citation. It is the product of a Gaussian that describes the metallicity distribution over halo stars and two Gaussians that describe the metallicity distribution in the thin and thick disks:

$$\begin{aligned} p(F) = & \quad H_F \frac{1}{\sqrt{2\pi\sigma^2_{\rm halo}}} \exp\left(-\frac{(F-\mu_{\rm halo})^2}{2\sigma_{\rm halo}}\right) \\ & \times (1 - H_F)\frac{1}{\xi}\left[\frac{0.8}{0.15}\exp\left(-\frac{(F-0.016)^2}{2\times 0.15^2}\right) + \frac{0.2}{0.22}\exp\left(-\frac{(F-0.15)^2}{2\times 0.22^2}\right)\right], \end{aligned} \tag{22}$$

where $H_F = 0.001$ is the halo fraction, $\mu_{\rm halo}$ and $\sigma_{\rm halo}$ are the mean and standard deviation of a Gaussian that describes a probability distribution over metallicity in the halo, and take values -1.5 and 0.4 respectively. The two Gaussians inside the square brackets describe probability distributions over metallicity in the thin and thick disks. The values of the means and standard deviations in these Gaussians are from **?**. ξ is the integral of everything in the square brackets from $-\infty$ to ∞ and takes the value ~ 2.507. The prior over distance is,

$$p(D) = \frac{3}{3000^3} D^2, \quad 0 < D < 3000, \tag{23}$$

where D is in kiloparsecs. Finally, the prior over extinction is uniform between zero and one,

$$p(A_V) = U(0, 1). \tag{24}$$

Some of the data presented in this paper were obtained from the Mikulski Archive for Space Telescopes (MAST). STScI is operated by the Association of Universities for Research in Astronomy, Inc., under NASA contract NAS5-26555. Support for MAST for non-HST data is provided by the NASA Office of Space Science via grant NNX09AF08G and by other grants and contracts. This paper includes data collected by the Kepler mission. Funding for the Kepler mission is provided by the NASA Science Mission directorate.

REFERENCES

R. Angus, S. Aigrain, D. Foreman-Mackey, and A. McQuillan. Calibrating gyrochronology using Kepler asteroseismic targets. *MNRAS*, 450:1787–1798, June 2015. doi: 10.1093/mnras/stv423.

S. A. Barnes. On the Rotational Evolution of Solar- and Late-Type Stars, Its Magnetic Origins, and the Possibility of Stellar Gyrochronology. *ApJ*, 586:464–479, March 2003. doi: 10.1086/367639.

S. A. Barnes. Ages for Illustrative Field Stars Using Gyrochronology: Viability, Limitations, and Errors. *ApJ*, 669:1167–1189, November 2007. doi: 10.1086/519295.

L. Casagrande and D. A. VandenBerg. On the use of Gaia magnitudes and new tables of bolometric corrections. *MNRAS*, 479:L102–L107, September 2018. doi: 10.1093/mnrasl/sly104.

W. J. Chaplin, S. Basu, D. Huber, et al. Asteroseismic Fundamental Properties of Solar-type Stars Observed by the NASA Kepler Mission. *ApJS*, 210:1, January 2014. doi: 10.1088/0067-0049/210/1/1.

C. R. Epstein and M. H. Pinsonneault. How Good a Clock is Rotation? The Stellar Rotation-Mass-Age Relationship for Old Field Stars. *ApJ*, 780:159, January 2014. doi: 10.1088/0004-637X/780/2/159.

S. D. Kawaler. Rotational dating of middle-aged stars. *ApJ*, 343:L65–L68, August 1989. doi: 10.1086/185512.

A. Skumanich. Time Scales for CA II Emission Decay, Rotational Braking, and Lithium Depletion. *ApJ*, 171:565, February 1972. doi: 10.1086/151310.

J. L. van Saders, T. Ceillier, T. S. Metcalfe, V. Silva Aguirre, M. H. Pinsonneault, R. A. García, S. Mathur, and G. R. Davies. Weakened magnetic braking as the origin of

anomalously rapid rotation in old field stars. *Nature*, 529:181–184, January 2016. doi: 10.1038/nature16168.